Feeling better: Separate pathways for targeted enhancement of spatial and temporal touch

Jeffrey M. Yau[1], **Pablo Celnik**[1,2,3], **Steven S. Hsiao**[2,4], and **John E. Desmond**[1,2]

[1]Department of Neurology, Johns Hopkins Medical Institutions, Baltimore, Maryland 21205, USA.

[2]Solomon H. Snyder Department of Neuroscience, Johns Hopkins Medical Institutions, Baltimore, Maryland 21205, USA.

[3]Department of Physical Medicine and Rehabilitation, Johns Hopkins Medical Institutions, Baltimore, Maryland 21231, USA.

[4]Zanvyl Krieger Mind/Brain Institute, Baltimore, Maryland 21218, USA.

Abstract

We perceive spatial form and temporal frequency by touch. Although distinct somatosensory neurons represent spatial and temporal information, these neural populations are intermixed throughout the somatosensory system. Here, we show that spatial and temporal touch can be dissociated and separately enhanced via cortical pathways that are normally associated with vision and audition. In Experiments 1 and 2, we found that anodal transcranial direct current stimulation (tDCS) applied over visual cortex, but not auditory cortex, enhances tactile perception of spatial orientation. In Experiments 3 and 4, we found that anodal tDCS over auditory cortex, but not visual cortex, enhances tactile perception of temporal frequency. This double-dissociation reveals separate cortical pathways that selectively support spatial and temporal channels. These results bolster the emerging view that sensory areas process multiple modalities and suggest that supramodal domains may be more fundamental to cortical organizational.

Keywords

Introduction

We have a remarkable capacity to perceive and understand our environment through our sense of touch alone (Hollins, 2010). With our hands, we perceive fine spatial information, like Braille dot patterns. We also perceive temporal information, in the form of vibrations, and this sensitivity underlies our appreciation of surface texture (Weber et al., in press). Separate receptors and afferent populations support spatial and temporal tactile channels in the peripheral somatosensory system (Johnson, 2001). Spatial and temporal tactile

information is also clearly represented in human primary and secondary somatosensory cortex (Burton, Sinclair, & McLaren, 2008; Burton, Sinclair, Wingert, & Dierker, 2008; Hegner, Lee, Grodd, & Braun, 2010; Kitada et al., 2006). Notably, the neural populations mediating spatial and temporal tactile channels are intermixed anatomically throughout the somatosensory system.

Tactile perception may also rely on neural processing in brain regions outside of the traditional somatosensory areas. Robust crossmodal tactile recruitment of visual cortex (VC) and auditory cortex (AC) is observed in the blind (Cohen et al., 1997; Pietrini et al., 2004; Sadato et al., 1996) and deaf (Auer, Bernstein, Sungkarat, & Singh, 2007; Levanen, Jousmaki, & Hari, 1998), and these cortical regions appear to retain their specialized functions in service of tactile perception (Merabet & Pascual-Leone, 2010). Interestingly, VC (Amedi, Malach, Hendler, Peled, & Zohary, 2001; James et al., 2002; Pietrini et al., 2004) and AC (Foxe et al., 2002; Kayser, Petkov, Augath, & Logothetis, 2005; Nordmark, Pruszynski, & Johansson, 2012; Schurmann, Caetano, Hlushchuk, Jousmaki, & Hari, 2006) can also respond to touch alone in sighted and normal hearing individuals, raising the possibility that crossmodal recruitment of sensory cortices may be a more ubiquitous mode of brain function rather than the consequence of sensory deprivation (Ghazanfar & Schroeder, 2006). If VC and AC contribute specifically to spatial and temporal touch, respectively, then these sensory regions might also be considered supramodal processors that support particular cognitive functions regardless of input modality, rather than as dedicated processors for a single modality (Ricciardi & Pietrini, 2011). According to this hypothesis, VC and AC would provide distinct crossmodal pathways for engaging spatial and temporal tactile channels.

The relationship between brain activity and behavior can be directly tested using non-invasive brain stimulation techniques like transcranial magnetic stimulation (TMS) and transcranial direct current stimulation (tDCS). Targeted enhancement or disruption of neural activity can acutely affect motor, sensory, and cognitive processes and can also induce specific functional changes that persist after the cessation of stimulation (Cohen Kadosh, Levy, O'Shea, Shea, & Savulescu, 2012; Nitsche et al., 2008; Nitsche & Paulus, 2011). In the sensory domain, both spatial and temporal touch are modulated by tDCS application over somatosensory cortex (Song, Sandrini, & Cohen, 2011). Here, we adopted tDCS strategies used for modulating visual and auditory function to investigate the contributions of visual and auditory areas to spatial and temporal touch. According to the supramodal organization hypothesis, we predicted that anodal tDCS over these regions would result in dissociable effects on touch (Fig. 1). In Experiments 1 and 2 we predicted that spatial touch would be enhanced by anodal tDCS over VC, but not AC. Conversely, in Experiments 3 and 4 we predicted that temporal touch would be enhanced by anodal tDCS over AC, but not VC.

General Method

General study design

Our study comprised four experiments based on a 2 × 2 factorial design crossing psychophysical task and tDCS site. For each experiment, we employed a counterbalanced, crossover design (Fig. 1*a*) with each participant receiving both anodal and sham tDCS in separate sessions. During each session, participants performed psychophysical tasks before ('Pre'), during ('Stim'), and after ('Post1' and 'Post2') receiving 20 min of tDCS intervention. On average, each participant's anodal and sham sessions were separated by one week. This design allowed us to quantify psychophysical performance changes that occurred during each session and to perform within-subject comparisons of perceptual changes specific to tDCS intervention.

Transcranial direct current stimulation

Anodal tDCS was delivered through 2 sponge electrodes (single electrode surface area: 25 cm^2) soaked in saline solution. In all experiments, the anodal (active) electrode was positioned according to International 10-20 EEG coordinates to target visual or auditory regions (see below) and the cathodal electrode was positioned on the right cheek over the buccinator muscle. We used these electrode montages (specifically, positioning the reference electrode over the right cheek) to avoid potential confounding effects of cathodal stimulation depressing cortical excitability beneath the reference electrode, as in other montages (Nitsche et al., 2008). Stimulation was delivered using the Chattanooga Iontophoresis System (Chattanooga Medical Supply, Inc, Chattanooga, TN), at current intensities that have been shown to be effective for modulating visual and auditory processing (see below). At the onset of anodal and sham stimulation, current increased in a ramp-like fashion over 30 s, a procedure shown to blind subjects effectively as to whether they received sham or non-sham stimulation (Gandiga, Hummel, & Cohen, 2006). Participants' ratings on attention, fatigue, and pain levels confirmed that their experiences of sham and anodal tDCS were statistically matched (Table 1).

Experiments 1 and 2

In these experiments we tested the contributions of visual and auditory brain regions to spatial touch: Participants performed a psychophysical task designed to measure tactile spatial acuity. In separate participant groups, we targeted visual cortex (Experiment 1) and auditory cortex (Experiment 2) for tDCS administration, and we adopted electrode positions used by previous studies to effectively modulate visual and auditory processing. For anodal tDCS administration over visual cortex (Fig. 1*b*), the anodal electrode was centered over the Oz site and current intensity was set at 1 mA (Antal, Kincses, Nitsche, Bartfai, & Paulus, 2004; Antal, Nitsche, & Paulus, 2001). Anodal tDCS over this site improves visual sensitivity to Gabor patches (Antal et al., 2001), which are visual analogues to the tactile grating stimuli we tested. For anodal tDCS administration over auditory cortex (Fig. 1*c*), the anodal electrode was centered over the T3 site and current intensity was set at 2 mA according to tDCS procedures previously used to improve auditory perceptual sensitivity (Ladeira et al., 2011). Given our additional interest in temporal touch (Experiments 3 and 4), we specifically targeted the left hemisphere for AC stimulation because frequency-dependent tactile responses have been shown to be lateralized to the left AC in humans, regardless of the hand stimulated (Nordmark et al., 2012).

Participants

Fifteen subjects (6 males; mean age = 25.2 ± 1.8 years; mean inter-session interval = 7.7 ± 0.99 days) participated in Experiment 1. A separate group of fifteen subjects (7 males; mean age = 22.5 ± 0.8 years; mean inter-session interval = 7.9 ± 1.04 days) participated in Experiment 2. All testing procedures were performed in compliance with the policies and procedures of the Johns Hopkins Institutional Review Board. All subjects gave their informed consent and were paid for their participation.

Method

Tactile spatial acuity was measured using a grating orientation identification task (Van Boven & Johnson, 1994; Werhahn, Mortensen, Van Boven, Zeuner, & Cohen, 2002; Zangaladze, Epstein, Grafton, & Sathian, 1999). Participants identified the orientation of tactile gratings centered on the distal finger pad of their left index finger. Gratings were either vertical or horizontal with respect to the finger's long axis and varied in grating width (GW; spatial period) from 0.5–3.0 mm (see Supplemental Material for a complete

description of the Grating Orientation Task). Orientation identification is easy with large GW values, but becomes more difficult at smaller GW levels.

Individual grating orientation thresholds were defined as the GW that corresponded to 75% correct performance and were determined by interpolating between GWs spanning 75% correct responses (unless performance was precisely at 75% correct response rate). This performance level is halfway between perfect and chance performance and is a standard psychophysical threshold criterion (corresponding to a d' value of 1.35).

Group grating orientation thresholds (inset in Fig. 2*a*) were derived by fitting the following psychometric function to performance data collapsed across all participants:

$$P(C) = 0.5 + \frac{0.5}{\left(1 + e^{-\frac{(GW - \alpha)}{\beta}}\right)}$$

where $p(C)$ is the proportion of correct responses, GW is grating width, α and β are free parameters, and the group threshold was the grating width corresponding to 75% correct performance along each psychometric curve. The resulting sigmoid functions range from 0.5 (chance performance) to 1 (perfect performance). Group thresholds revealed an effects pattern that closely resembled the average pattern of thresholds calculated for individual participants. All statistical analyses were performed on grating orientation thresholds estimated for individual participants.

Data analysis

All statistical tests were performed using Matlab. To determine whether grating orientation thresholds changed as a function of tDCS we conducted repeated-measures ANOVA with time ('Pre', 'Stim', and 'Post1') and tDCS (anodal and sham) as *within-subjects* factors. We performed *post hoc* paired t-tests (Bonferroni corrected) if ANOVA interaction effects reached statistical significance. To characterize the persistence of tDCS effects, we conducted planned comparison paired t-tests assessing whether dependent measures in the 'Post2' block differed from values in the 'Pre' block. To determine whether baseline thresholds depended on session order (which would reveal carryover effects between sessions) we conducted repeated-measures ANOVA with 'Pre' estimates as the dependent measure and session number (session 1 and session 2) and tDCS (anodal and sham) as *within-subjects* factors.

Results

In Experiment 1, participants identified the orientation of tactile gratings presented to their finger before, during, and following application of anodal tDCS over VC (Fig. 1*b*). We found that grating orientation thresholds decreased significantly with anodal tDCS (Fig. 2*a,b*) (ANOVA$_{RM}$: time x tDCS interaction, $F_{(2,27)} = 3.7$, $p = 0.03$, $\eta_p^2 = 0.207$) and improved spatial acuity was clearly evident in individual subjects (Fig. 2*c*). Average thresholds following anodal stimulation were significantly lower compared to baseline thresholds (Post1$_A$ vs Pre$_A$; $t_{(14)} = 3.65$, $p = 0.003$, $d = 0.89$) and compared to thresholds following sham intervention (Post1$_A$ vs Post1$_S$; $t_{(14)} = 2.76$, $p = 0.008$, $d = 0.93$). Critically, baseline thresholds did not differ between anodal and sham sessions (Pre$_A$ vs Pre$_S$; $t_{(14)} = 0.63$, $p = 0.73$), indicating that the magnitude of perceptual enhancements did not depend on participants' initial sensitivities in test sessions. Baseline thresholds did not depend on session order (two-way ANOVA: session and tDCS, main and interaction effect $ps > 0.09$), showing that perceptual enhancements did not carryover between sessions. Thresholds

measured 15 min after tDCS cessation rebounded, but remained lower than baseline (Post2$_A$ vs Pre$_A$; $t_{(14)} = 2.2$, $p = 0.04$, $d = 0.5$). Together, these results indicate that anodal tDCS over VC induces robust, but temporary, improvements in tactile spatial perception.

In contrast to Experiment 1 results, grating orientation thresholds were unaffected by anodal tDCS over AC (Fig. 2d,e). Although baseline thresholds in Experiment 2 were comparable to Experiment 1 baselines, spatial acuity estimates remained unchanged during test sessions and did not differ between anodal and sham sessions (Fig. 2e) (time and tDCS, main and interaction effect $ps > 0.14$). Accordingly, while there was again substantial performance variability across participants (Fig. 2f), the dispersion in participants' thresholds did not reveal bias toward improved spatial acuity in anodal sessions. Thus, application of anodal tDCS over VC, but not AC, results in improved spatial touch.

Experiments 3 and 4

In these experiments we tested the contributions of auditory and visual brain regions to temporal touch: Participants performed a psychophysical task designed to measure vibration frequency sensitivity. In separate participant groups, we targeted auditory cortex (Experiment 3) and visual cortex (Experiment 4) for tDCS administration, using the same tDCS methods as those used in Experiments 1 and 2 with the exception that current intensity was set to 2 mA for both stimulation sites.

Participants

Fifteen subjects (5 males; mean age = 25.3 ± 0.7 years; mean inter-session interval = 9 ± 0.8 days) participated in Experiment 3 (4 had participated in Experiment 1 and 2 had participated in Experiment 2). A separate group of fifteen subjects (6 males; mean age = 23.8 ± 1.2 years; mean inter-session interval = 8.1 ± 0.7 days) participated in Experiment 4. All testing procedures were performed in compliance with the policies and procedures of the Johns Hopkins Institutional Review Board. All subjects gave their informed consent and were paid for their participation.

Method

Tactile frequency sensitivity was assessed using a frequency discrimination task (Yau, Olenczak, Dammann, & Bensmaia, 2009). Participants judged which of two vibrotactile stimuli, delivered sequentially to the participant's left index finger, was perceived as being higher in frequency. One trial interval always contained a 3009Hz vibration (standard stimulus); the frequency of the vibration presented during the other interval (comparison stimulus) ranged from 150 to 450 Hz in 509Hz increments (excluding 300 Hz). Vibration stimuli were equated in perceived intensity to ensure that participants could only perform the discrimination task using frequency information (see Supplemental Material for a complete description of the Frequency Discrimination Task).

To quantify participants' ability to discriminate frequency, we fit each participant's data with a psychometric function:

$$p(f_C > f_S) = \frac{1}{1 + e^{-\frac{(f_c - \mu)}{\sigma}}}$$

where $p(f_c > f_S)$ is the proportion of trials a comparison stimulus with frequency f_C was judged to be higher in frequency than the standard stimulus with frequency f_S, and σ and μ are free parameters corresponding to estimates of the participant's sensitivity and bias,

respectively. Sensitivity estimates denote the change in frequency (with respect to the standard) that participants could detect 73% of the time. Bias estimates indicate the point of subjective equality. The resulting sigmoid ranges from 0 to 1. Psychometric functions were also fit to the aggregated group data for illustration purposes (Fig. 3a,d), but all statistical tests were conducted on the parameters estimated for individual subjects.

To quantify the change in each participant's frequency sensitivity (improvement rates), we fit sensitivity estimates in each session with an exponential function:

$$S(t) = S_0 e^{-\lambda t}$$

where $S(t)$ is the sensitivity estimate (σ) at time t, S_0 denotes baseline sensitivity, and λ is the improvement rate. We modeled improvement rates with an exponential function because sensitivity estimates were necessarily greater than zero (and the function captured decay toward this theoretical lower bound). For completeness, we confirmed that improvement rates based on linear functions yielded similar results. To increase the time points included in the temporal function fits and to detect improvement within test blocks, functions were fit to sensitivity values estimated separately from performance data in the first and second half of each test block (8 sensitivity values per session). A similar pattern of results was seen with rate estimates fit to all of the performance data within each test block (4 sensitivity values per session).

All parameter estimations and statistical analyses were performed using Matlab (Mathworks). Psychometric functions were fit to each participant's performance data using an iterative nonlinear least-squares algorithm (lsqnonlin) to minimize the sum of squared differences between observed and predicted performance levels. To determine whether sensitivity parameters changed as a function of tDCS we conducted repeated-measures ANOVA with time ('Pre', 'Stim', and 'Post1') and tDCS (anodal and sham) as *within-subjects* factors. We conducted one-sample t-tests to determine the significance of sensitivity improvement rates and paired t-tests to determine whether improvement rates differed according to tDCS intervention.

Results

In Experiment 3, participants performed a tactile frequency discrimination task during sessions in which they received tDCS over AC (Fig. 1c). Across the participant group, frequency sensitivity improved significantly during test sessions (Fig. 3a,b; lower σ values indicate better frequency sensitivity) (time main effect, $F_{(2,27)} = 5.29$, $p = 0.01$, $\eta_p^2 = 0.153$) and substantial sensitivity changes were evident in individual subjects (Fig. 3c). Bias estimates were unaffected by tDCS (time and tDCS, main and interaction effect $ps > 0.55$). Although participants were significantly more sensitive to vibration frequency during anodal sessions (tDCS main effect, $F_{(1,27)} = 8.34$, $p = 0.01$, $\eta_p^2 = 0.187$), the time x tDCS interaction effect failed to reach significance ($F_{(2,27)} = 1.59$, $p = 0.22$). This result was due to the fact that frequency sensitivity also improved modestly during sham sessions, which suggests a general practice or learning effect with the frequency task. Indeed, we also found that response times improved over the course of testing (time main effect, $F_{(3,42)} = 6.98$, $p = 0.0007$, $\eta_p^2 = 0.491$), during both anodal and sham sessions (tDCS main effect $p = 0.66$; time x tDCS interaction $p = 0.21$). Together, these results reveal that participants' performance on the vibration frequency task improved generally within test sessions; however, the greater overall sensitivity during anodal sessions suggests that the general improvements may have been enhanced by tDCS over AC.

We quantified and compared the rate of sensitivity improvement during anodal and sham sessions (Fig. 3b, inset). Rate estimates (λ) revealed significant improvements in frequency sensitivity during both anodal ($t_{(14)} = 4.15$, $p = 0.0009$) and sham sessions ($t_{(14)} = 2.51$, $p = 0.025$), consistent with general practice or learning effects. Critically, though, rate estimates were significantly larger for anodal sessions ($t_{(14)} = 2.56$, $p = 0.02$, $d = 0.84$), indicating that anodal stimulation over AC enhanced performance gains on the tactile frequency discrimination task relative to sham.

In Experiment 4, we found that tDCS over VC did not significantly modulate sensitivity estimates (time and tDCS, main and interaction effect $ps > 0.17$) (Fig. 3d,e). Bias estimates also did not vary over sham and anodal sessions (time and tDCS, main and interaction effect $ps > 0.48$). Although the psychophysical parameters were not significantly modulated by tDCS or time, participants did show general performance gains during test sessions, as measured by faster response times ($F_{(3,42)} = 9.06$, $p = 0.0001$, $\eta_p^2 = 0.346$). Analysis of improvement rates also revealed general performance gains (Fig. 3e, inset): Significant rates were observed in sham ($t_{(14)} = 3.59$, $p = 0.003$) and anodal sessions ($t_{(14)} = 2.93$, $p = 0.01$), but these effects did not differ between sham and anodal tDCS interventions ($t_{(14)} = 0.9$, $p = 0.38$). The equivalence between sham and anodal tDCS effects in Experiment 4 is also obvious from the sensitivity data for individual subjects (Fig. 3f): While frequency sensitivity in some participants improved, there was no evidence for greater or more consistent improvement during anodal sessions compared to sham over the group. Together, the results of Experiments 3 and 4 indicate that anodal tDCS over AC, but not VC, can facilitate performance gains on a vibration discrimination task, resulting in larger improvements in frequency sensitivity.

Discussion

We sought to identify separate crossmodal mechanisms for spatial and temporal touch and we found that anodal tDCS over visual and auditory regions dissociates between these perceptual channels. Tactile perception of grating orientation improved with anodal tDCS over VC, but not AC. Conversely, anodal tDCS over AC, but not VC, resulted in greater improvements in sensitivity to vibration frequency.

Acute application of anodal tDCS enhances neuronal excitability by inducing a tonic depolarization of resting membrane potential (Cohen Kadosh et al., 2012; Nitsche et al., 2008). Increased cortical excitability, resulting in increased neural signal relative to noise, may have resulted in the rapid sensitivity changes we observed during tDCS application ('Stim' block) in Experiments 1 and 3. In comparison, the persistence of tactile sensibility improvements beyond the stimulation period likely resulted from an interaction between anodal tDCS and performance of the psychophysical tasks. Indeed, prolonged application of anodal tDCS can induce neuroplasticity resembling activity-dependent long-term potentiation (LTP) (Fritsch et al., 2010; Nitsche & Paulus, 2011), and anodal tDCS appears to benefit human motor learning when stimulation is paired with training (Reis et al., 2009). In our experiments, the coincidence of task performance with tDCS administration may have served to restrict potentiation effects to the neural populations specifically engaged in crossmodal processing or perceptual learning, leading to the persistent sensitivity improvements. Even extensive practice without brain stimulation can result in improvements in spatial (Wong, Peters, & Goldreich, 2013) and temporal (Imai et al., 2003) touch, so anodal tDCS interventions likely facilitate processing in cortical circuits that typically undergo experience-dependent plasticity. Whether comparable perceptual gains can be achieved with anodal tDCS alone remains to be tested. Critically, while experience- or stimulation-induced augmentation of central processes may increase perceptual sensitivity,

the range of gains is still ultimately constrained by the response properties of peripheral afferent populations (Johnson, 2001; Van Boven & Johnson, 1994).

What specific brain regions were influenced by tDCS in our experiments? Current distribution and focality with tDCS can vary depending on the arrangement and size of the stimulating electrodes (Nitsche et al., 2008; Nitsche & Paulus, 2011). In our electrode montages, cortical tissue resided beneath only the anodal (active) electrode, restricting neuromodulatory effects to the targeted cortical regions. Modeling studies indicate that current density along the cortical surface, only a fraction of the total injected current due to substantial shunting through the scalp (Wagner et al., 2007), is relatively homogenous over restricted areas directly under the electrode (Miranda, Lomarev, & Hallett, 2006). Thus, with the EEG coordinate targets we adopted (Fig. 1*b,c*), we are confident that our tDCS interventions affected visual regions (in Experiments 1 and 4) and auditory regions (in Experiments 2 and 3); however, we cannot definitively rule out that other neighboring areas were also stimulated. For instance, anodal tDCS over the Oz site, which enhances visual sensitivity (Antal et al., 2001), may modulate cortical excitability in primary or association visual areas (i.e., striate and extrastriate cortex). Similarly, anodal tDCS over the T3 site, which enhances auditory sensitivity (Ladeira et al., 2011), may modulate cortical responses in primary or association auditory areas (i.e., core, belt, and parabelt regions). Furthermore, tDCS over the T3 site, which enhanced frequency sensitivity in Experiment 3, may have also modulated neural responses in secondary somatosensory cortex (S2), especially given that parietal operculum (PO), the human homologue of monkey S2, exhibits responses to high-frequency vibrations (Burton, Sinclair, & McLaren, 2008; Burton, Sinclair, Wingert, et al., 2008). Critically, PO also responds to tactile spatial patterns (Burton, Sinclair, Wingert, et al., 2008; Hegner et al., 2010; Kitada et al., 2006). Thus, it is conceivable that tDCS affecting S2 would influence both spatial and temporal touch; however, no spatial touch enhancement was observed in Experiment 2. Therefore, given the limited focality of tDCS, we cannot claim that tDCS over T3 modulated only auditory brain regions, but we can conclude that tDCS over this site dissociates temporal touch from spatial touch.

That tDCS over VC and AC influences tactile processing is consistent with neuroimaging studies employing methods that are suited for localizing tactile responses to visual brain regions (Amedi et al., 2001; James et al., 2002; Pietrini et al., 2004) and auditory brain regions (Foxe et al., 2002; Kayser et al., 2005; Schurmann et al., 2006). Notably, left AC exhibits frequency-dependent tactile responses for sinusoidal stimulation of either the left or right hand (Nordmark et al., 2012) and our results suggest that the asymmetric specialization of human AC (i.e., left AC for fundamental pitch processing and right AC for spectral processing (Warrier et al., 2009)) may extend to crossmodal frequency processing – this generalization, though, remains to be tested systematically in future studies.

In addition to neuroimaging studies, our results also corroborate the findings of disruptive brain stimulation studies (Bolognini, Papagno, Moroni, & Maravita, 2010; Merabet et al., 2004; Zangaladze et al., 1999) that support the supramodal organization hypothesis. Notably, because we find that tactile sensibilities are enhanced following VC and AC stimulation, our study additionally establishes the clinical potential of crossmodal tDCS interventions for sensory rehabilitation and perceptual enhancement (Cohen Kadosh et al., 2012).

Because non-invasive brain stimulation targeting classically-defined somatosensory regions also modulates perception of spatial and temporal tactile stimulus features (Song et al., 2011), we propose that tactile perception is supported by distributed cortical networks that comprise somatosensory areas cooperating with visual and auditory areas. Anatomical connectivity studies have identified several pathways by which information potentially

transfers between sensory systems (Cappe, Rouiller, & Barone, 2012). A key question yet to be addressed is how connectivity in these distributed networks is dynamically modulated and maintained. Potentially, deployment of selective attention to particular stimulus features, like grating orientation or vibration frequency, enhances somatosensory connectivity with VC or AC, respectively. Cross-areal coupling may be achieved by synchronizing intrinsic brain oscillations in these cortical networks (Canolty & Knight, 2010), and this mechanism has been shown to amplify selected sensory information (Schroeder & Lakatos, 2009).

In summary, common cortical resources appear to support spatial form and temporal frequency processing across sensory modalities. Shared processing mechanisms can account for correspondences in haptic and visual shape perception (Lacey & Sathian, 2011) and in haptic and auditory frequency perception (Bensmaia, Hollins, & Yau, 2005). Multisensory convergence in common cortical processors also predicts highly specific somatosensory interactions with vision (Lacey & Sathian, 2011) and audition (Yau, Weber, & Bensmaia, 2010). However, it is important to note that supramodal processors may not explain all interactions between sensory modalities, as multisensory interplay is not necessarily restricted to specific feature dimensions. Nevertheless, our results bolster the emerging view that sensory areas are not dedicated to single modalities and suggest that cortical organization can be defined by supramodal perceptual domains.

Acknowledgments

References

Amedi A, Malach R, Hendler T, Peled S, Zohary E. Visuo-haptic object-related activation in the ventral visual pathway. Nature Neuroscience. 2001; 4:324–330.

Antal A, Kincses TZ, Nitsche MA, Bartfai O, Paulus W. Excitability changes induced in the human primary visual cortex by transcranial direct current stimulation: direct electrophysiological evidence. Invest Ophthalmol Vis Sci. 2004; 45(2):702–707. [PubMed: 14744917]

Antal A, Nitsche MA, Paulus W. External modulation of visual perception in humans. Neuroreport. 2001; 12(16):3553–3555. [PubMed: 11733710]

Auer ET Jr. Bernstein LE, Sungkarat W, Singh M. Vibrotactile activation of the auditory cortices in deaf versus hearing adults. Neuroreport. 2007; 18(7):645–648. [PubMed: 17426591]

Bensmaia S, Hollins M, Yau J. Vibrotactile intensity and frequency information in the pacinian system: a psychophysical model. Perception and Psychophysics. 2005; 67:828–841. [PubMed: 16334055]

Bolognini N, Papagno C, Moroni D, Maravita A. Tactile temporal processing in the auditory cortex. J Cogn Neurosci. 2010; 22(6):1201–1211. [PubMed: 19413471]

Burton H, Sinclair RJ, McLaren DG. Cortical network for vibrotactile attention: a fMRI study. Hum Brain Mapp. 2008; 29(2):207–221. [PubMed: 17390318]

Burton H, Sinclair RJ, Wingert JR, Dierker DL. Multiple parietal operculum subdivisions in humans: tactile activation maps. Somatosens Mot Res. 2008; 25(3):149–162. [PubMed: 18821280]

Canolty RT, Knight RT. The functional role of cross-frequency coupling. Trends Cogn Sci. 2010; 14(11):506–515. [PubMed: 20932795]

Cappe, C.; Rouiller, EM.; Barone, P. Cortical and Thalamic Pathways for Multisensory and Sensorimotor Interplay.. In: Murray, MM.; Wallace, MT., editors. The Neural Bases of Multisensory Processes. CRC Press; Boca Raton, FL: 2012.

Cohen Kadosh R, Levy N, O'Shea J, Shea N, Savulescu J. The neuroethics of non-invasive brain stimulation. Curr Biol. 2012; 22(4):R108–111. [PubMed: 22361141]

Cohen LG, Celnik P, Pascual-Leone A, Corwell B, Faiz L, Dambrosia J, Hallett M. Functional relevance of cross-modal plasticity in blind humans. Nature. 1997; 389:180–183. [PubMed: 9296495]

Foxe JJ, Wylie GR, Martinez A, Schroeder CE, Javitt DC, Guilfoyle D, Murray MM. Auditory-somatosensory multisensory processing in auditory association cortex: an fMRI study. Journal of Neurophysiology. 2002; 88:540–543. [PubMed: 12091578]

Fritsch B, Reis J, Martinowich K, Schambra HM, Ji Y, Cohen LG, Lu B. Direct current stimulation promotes BDNF-dependent synaptic plasticity: potential implications for motor learning. Neuron. 2010; 66(2):198–204. [PubMed: 20434997]

Gandiga PC, Hummel FC, Cohen LG. Transcranial DC stimulation (tDCS): a tool for double-blind sham-controlled clinical studies in brain stimulation. Clin Neurophysiol. 2006; 117(4):845–850. [PubMed: 16427357]

Ghazanfar AA, Schroeder CE. Is neocortex essentially multisensory? Trends Cogn Sci. 2006; 10(6): 278–285. [PubMed: 16713325]

Hegner YL, Lee Y, Grodd W, Braun C. Comparing tactile pattern and vibrotactile frequency discrimination: A human fMRI study. J Neurophysiol. 2010; 103:3115–3122. [PubMed: 20457848]

Hollins M. Somesthetic senses. Annu Rev Psychol. 2010; 61:243–271. [PubMed: 19575612]

Imai T, Kamping S, Breitenstein C, Pantev C, Lutkenhoner B, Knecht S. Learning of tactile frequency discrimination in humans. Hum Brain Mapp. 2003; 18(4):260–271. doi: 10.1002/hbm.10083. [PubMed: 12632464]

James TW, Humphrey GK, Gati JS, Servos P, Menon RS, Goodale MA. Haptic study of three-dimensional objects activates extrastriate visual areas. Neuropsychologia. 2002; 40(10):1706–1714. [PubMed: 11992658]

Johnson KO. The roles and functions of cutaneous mechanoreceptors. Current Opinion in Neurobiology. 2001; 11:455–461. [PubMed: 11502392]

Kayser C, Petkov CI, Augath M, Logothetis NK. Integration of touch and sound in auditory cortex. Neuron. 2005; 48:373–384. [PubMed: 16242415]

Kitada R, Kito T, Saito DN, Kochiyama T, Matsumura M, Sadato N, Lederman SJ. Multisensory activation of the intraparietal area when classifying grating orientation: a functional magnetic resonance imaging study. Journal of Neuroscience. 2006; 26:7491–7501. [PubMed: 16837597]

Lacey S, Sathian K. Multisensory object representation: insights from studies of vision and touch. Prog Brain Res. 2011; 191:165–176. [PubMed: 21741551]

Ladeira A, Fregni F, Campanha C, Valasek CA, De Ridder D, Brunoni AR, Boggio PS. Polarity-dependent transcranial direct current stimulation effects on central auditory processing. PLoS One. 2011; 6(9):e25399. [PubMed: 21966519]

Levanen S, Jousmaki V, Hari R. Vibration-induced auditory-cortex activation in a congenitally deaf adult. Current Biology. 1998; 8:869–872. [PubMed: 9705933]

Merabet LB, Pascual-Leone A. Neural reorganization following sensory loss: the opportunity of change. Nat Rev Neurosci. 2010; 11(1):44–52. [PubMed: 19935836]

Merabet L, Thut G, Murray B, Andrews J, Hsiao S, Pascual-Leone A. Feeling by sight or seeing by touch? Neuron. 2004; 42:173–179. [PubMed: 15066274]

Miranda PC, Lomarev M, Hallett M. Modeling the current distribution during transcranial direct current stimulation. Clin Neurophysiol. 2006; 117(7):1623–1629. [PubMed: 16762592]

Nitsche MA, Cohen LG, Wassermann EM, Priori A, Lang N, Antal A, Pascual-Leone A. Transcranial direct current stimulation: State of the art 2008. Brain Stimul. 2008; 1(3):206–223. [PubMed: 20633386]

Nitsche MA, Paulus W. Transcranial direct current stimulation--update 2011. Restor Neurol Neurosci. 2011; 29(6):463–492. [PubMed: 22085959]

Nordmark PF, Pruszynski JA, Johansson RS. BOLD responses to tactile stimuli in visual and auditory cortex depend on the frequency content of stimulation. J Cogn Neurosci. 2012; 24(10):2120–2134. [PubMed: 22721377]

Pietrini P, Furey ML, Ricciardi E, Gobbini MI, Wu WH, Cohen L, Haxby JV. Beyond sensory images: Object-based representation in the human ventral pathway. Proc Natl Acad Sci USA. 2004; 101:5658–5663. [PubMed: 15064396]

Reis J, Schambra HM, Cohen LG, Buch ER, Fritsch B, Zarahn E, Krakauer JW. Noninvasive cortical stimulation enhances motor skill acquisition over multiple days through an effect on consolidation. Proc Natl Acad Sci U S A. 2009; 106(5):1590–1595. [PubMed: 19164589]

Ricciardi E, Pietrini P. New light from the dark: what blindness can teach us about brain function. Curr Opin Neurol. 2011; 24(4):357–363. doi: 10.1097/WCO.0b013e328348bdbf. [PubMed: 21677583]

Sadato N, Pascual-Leone A, Grafman J, Ibanez V, Deiber MP, Dold GR, Hallett M. Activation of the primary visual cortex by Braille reading in blind subjects. Nature. 1996; 380(6574):526–528. [PubMed: 8606771]

Schroeder CE, Lakatos P. Low-frequency neuronal oscillations as instruments of sensory selection. Trends Neurosci. 2009; 32(1):9–18. [PubMed: 19012975]

Schurmann M, Caetano G, Hlushchuk Y, Jousmaki V, Hari R. Touch activates human auditory cortex. Neuroimage. 2006; 30:1325–1331. [PubMed: 16488157]

Song S, Sandrini M, Cohen LG. Modifying somatosensory processing with non-invasive brain stimulation. Restor Neurol Neurosci. 2011; 29(6):427–437. [PubMed: 22124034]

Van Boven RW, Johnson KO. The limit of tactile spatial resolution in humans: Grating orientation discrimination at the lip, tongue and finger. Neurology. 1994; 44:2361–2366. [PubMed: 7991127]

Wagner T, Fregni F, Fecteau S, Grodzinsky A, Zahn M, Pascual-Leone A. Transcranial direct current stimulation: a computer-based human model study. Neuroimage. 2007; 35(3):1113–1124. [PubMed: 17337213]

Warrier C, Wong P, Penhune V, Zatorre R, Parrish T, Abrams D, Kraus N. Relating structure to function: Heschl's gyrus and acoustic processing. J Neurosci. 2009; 29(1):61–69. doi: 10.1523/JNEUROSCI.3489-08.2009. [PubMed: 19129385]

Weber AI, Saal HP, Lieber JD, Cheng JW, Manfredi LR, Dammann JF, Bensmaia SJ. Spatial and temporal codes mediate the tactile perception of natural textures. Proceedings of the National Academy of Sciences of the United States of America. in press.

Werhahn KJ, Mortensen J, Van Boven RW, Zeuner KE, Cohen LG. Enhanced tactile spatial acuity and cortical processing during acute hand deafferentation. Nature Neuroscience. 2002; 5:936–938.

Wong M, Peters RM, Goldreich D. A physical constraint on perceptual learning: tactile spatial acuity improves with training to a limit set by finger size. J Neurosci. 2013; 33(22):9345–9352. doi: 10.1523/JNEUROSCI.0514-13.2013. [PubMed: 23719803]

Yau JM, Olenczak JB, Dammann JF, Bensmaia SJ. Temporal Frequency Channels Are Linked across Audition and Touch. Curr Biol. 2009; 19(7):561–566. [PubMed: 19268591]

Yau JM, Weber AI, Bensmaia SJ. Separate mechanisms for audio-tactile pitch and loudness interactions. Front Psychology. 2010; 1(160) doi: 10.3389/fpsyg.2010.00160.

Zangaladze A, Epstein CM, Grafton ST, Sathian K. Involvement of visual cortex in tactile discrimination of orientation. Nature. 1999; 401:587–590. [PubMed: 10524625]

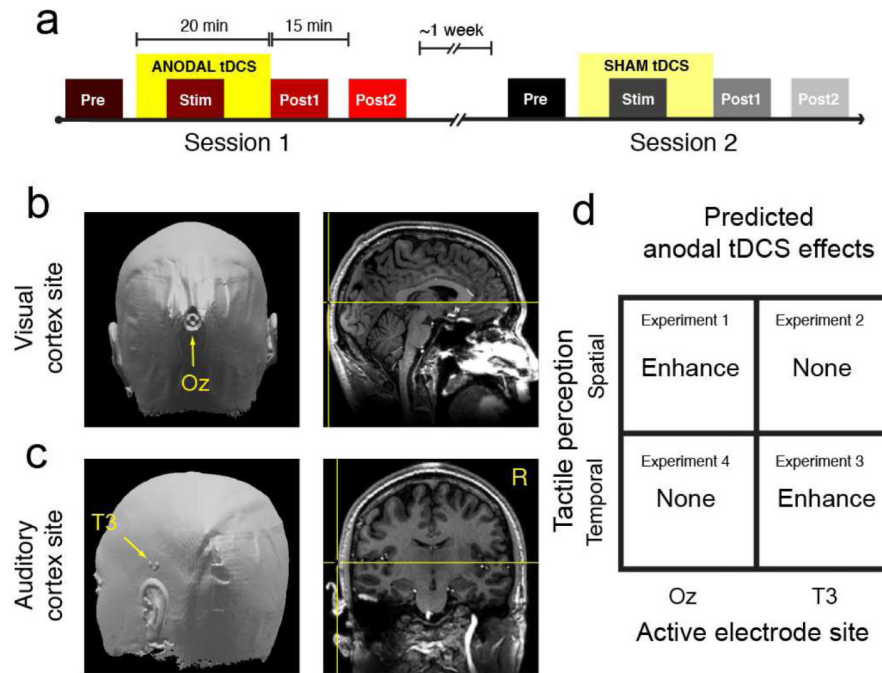**Figure 1. Experimental design**
(a) In each experiment, participants received 20 min of anodal tDCS (bright yellow box) or sham tDCS (faint yellow box) in 2 sessions separated by approximately 1 week. The order of tDCS treatment was counterbalanced across participants. Participants performed 4 blocks of discrimination trials ('Pre', 'Stim', 'Post1', and 'Post2') during anodal (red hued boxes) and sham (gray hued boxes) sessions. Testing during tDCS ('Stim') began 5 min after stimulation onset. Testing in the final block ('Post2') began 15 min after the cessation of tDCS. **(b)** Anodal electrode placement for stimulation over visual cortex identified by a fiducial marker in a high-resolution anatomical scan in one participant. The anodal electrode was positioned (over the Oz site) according to the International 10-20 EEG coordinate system. **(c)** Anodal electrode placement for stimulation over left auditory cortex, positioned over the T3 site. **(d)** Predicted tDCS effects on spatial and temporal touch for stimulation over visual and auditory cortex.
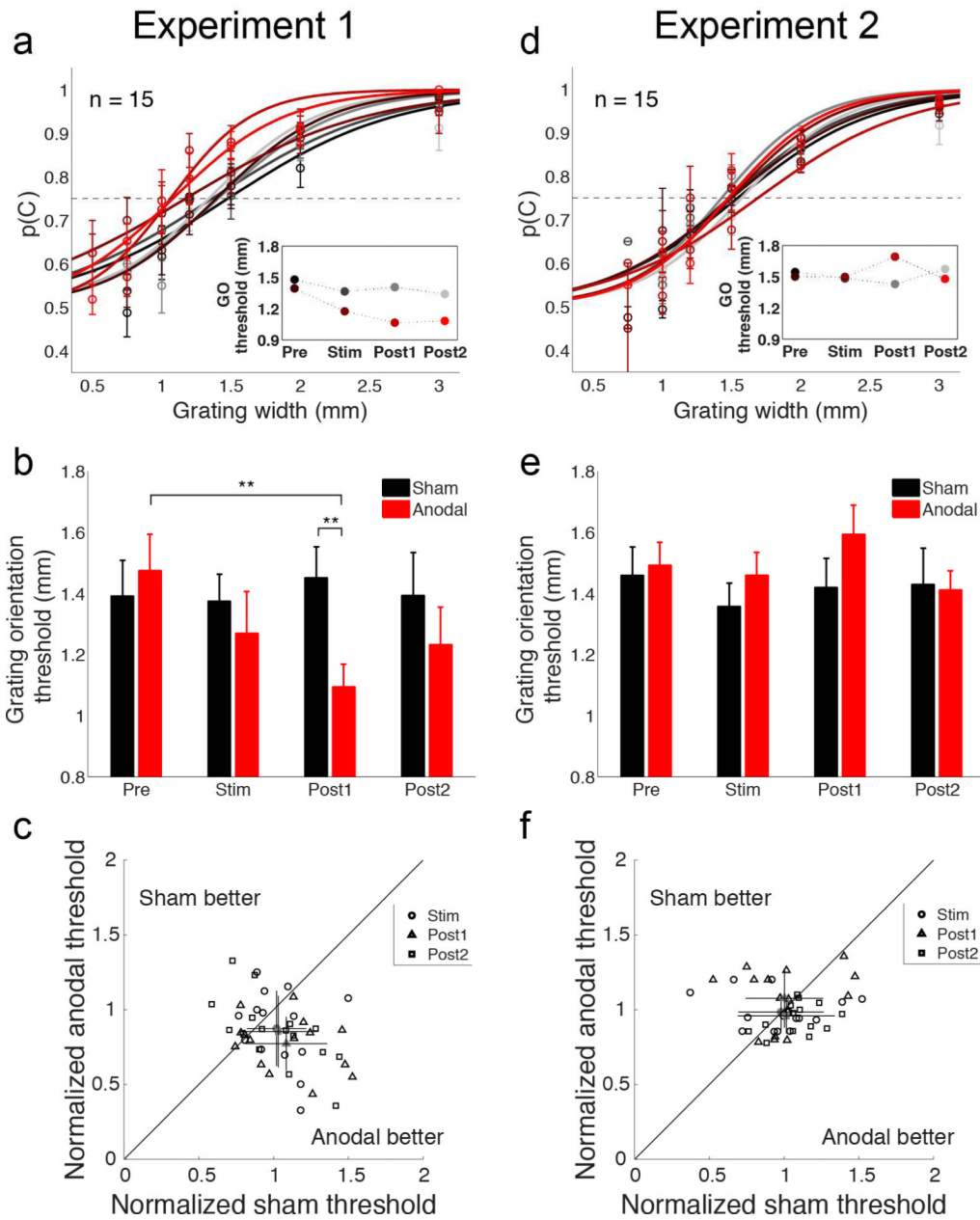
Figure 2. Results from Experiments 1 and 2

(a) Group psychometric curves (*n* = 15) from grating orientation discrimination task (Experiment 1; tDCS over Oz). Probability of correct orientation identification is plotted as a function of tactile grating width. Error bars indicate s.e.m. Curves are fit to data averaged over all participants. Separate performance curves are plotted for anodal blocks (red hues) and sham blocks (gray hues). Color coding as in Fig. 1*a*. Grating orientation (GO) threshold is taken as the grating width that yields 75% correct performance (dashed line). The leftward shift of performance curves indicates enhanced spatial acuity. Inset plot shows grating orientation thresholds estimated from group psychometric curves for each test block. **(b)** Average grating orientation thresholds calculated for individual participants during sham (black) and anodal (red) sessions. Tactile spatial acuity improved during anodal sessions but remained unchanged during sham sessions. Error bars indicate s.e.m. **, *p* < 0.01. **(c)**

Scatter plot shows the relationship between each participant's grating orientation thresholds in the sham and anodal sessions during 'Stim' (circles), 'Post1' (triangles), and 'Post2' (squares) test blocks. Thresholds are normalized by each participant's baseline ('Pre') threshold estimate for each session. Baseline-normalization accounts for across-session and across-subject variability. Average normalized thresholds (gray markers) reveal greater enhancement of tactile spatial acuity during anodal sessions. Error bars indicate standard deviation. **(d)** Group psychometric curves ($n = 15$) from grating orientation discrimination task (Experiment 2; tDCS over T3). Conventions as in (a). **(e)** Average grating orientation thresholds calculated for individual participants in Experiment 2. Tactile spatial acuity remained unchanged during sham and anodal sessions. **(f)** Scatter plot shows the relationship between each participant's grating orientation thresholds in sham and anodal sessions in Experiment 2. Conventions as in (c). Normalized thresholds showed no bias toward better spatial acuity with anodal tDCS over T3.
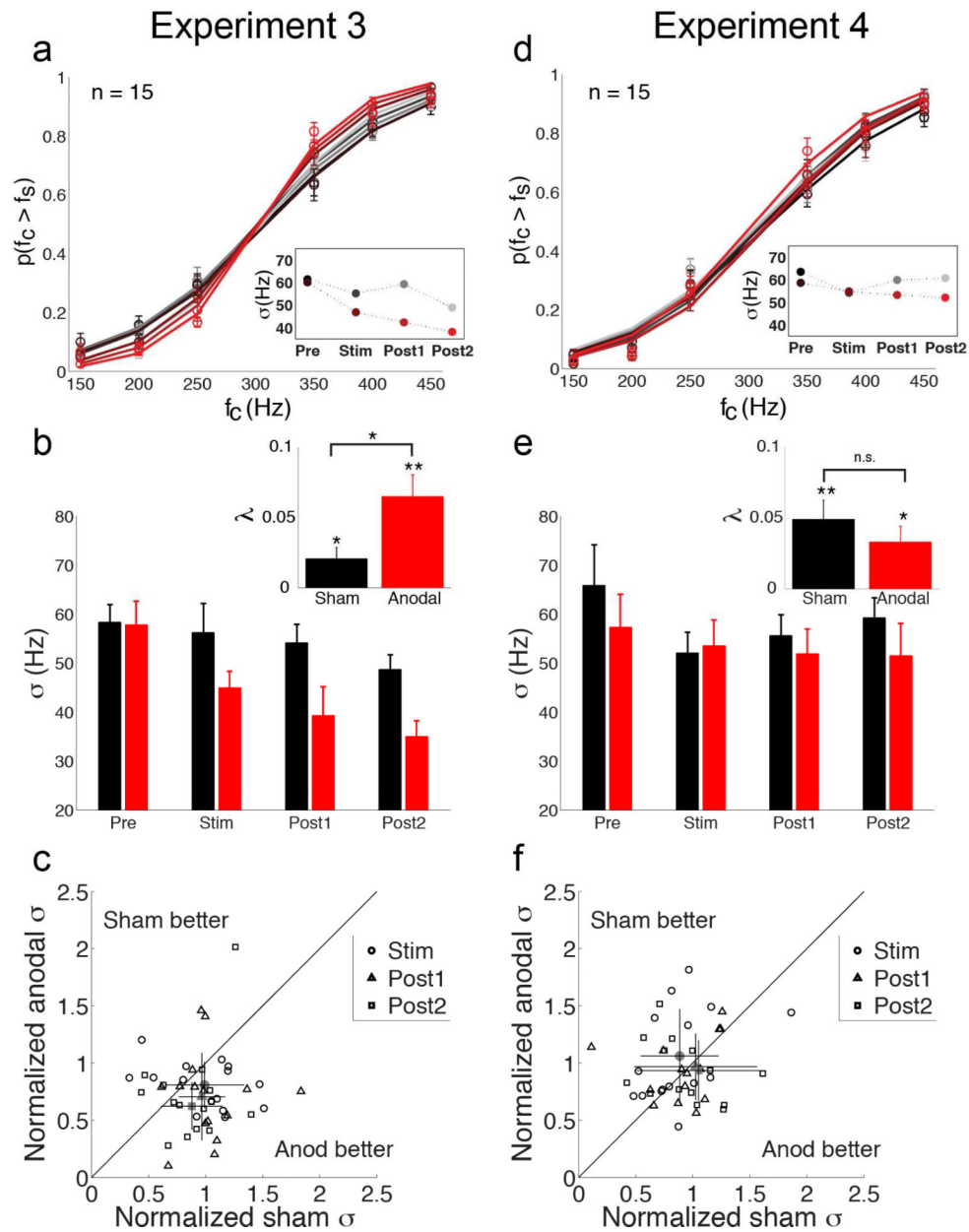
Figure 3. Results from Experiments 3 and 4

(**a**) Group psychometric curves ($n = 15$) from frequency discrimination task (Experiment 3; tDCS over T3). Data indicate probability that the frequency of a comparison stimulus (f_C) is judged to be higher than the frequency of the standard stimulus ($f_S = 300$Hz). Error bars indicate s.e.m. Curves are fit to data aggregated over all participants. Color coding as in Fig. 1*a*. Inset plot shows frequency sensitivity parameter (σ) estimated from the group psychometric curves for each test block. Smaller sigma values indicate high sensitivity. (**b**) Average frequency sensitivity estimates calculated for individual participants during sham (black) and anodal (red) sessions. Frequency sensitivity was significantly enhanced during anodal sessions compared to sham. Inset bar plots indicate sensitivity improvement rates (λ) over the course of sham (black) and anodal (red) sessions. Error bars indicate s.e.m. Larger lambda values indicate greater sensitivity improvement rates. Improvement rates were significantly greater during anodal sessions compared to sham. *, $p < 0.05$; **, $p < 0.01$. (**c**)

Scatter plot shows the relationship between each participant's frequency sensitivity estimates in the sham and anodal sessions during 'Stim' (circles), 'Post1' (triangles), and 'Post2' (squares) test blocks. Sensitivity estimates are normalized by each participant's baseline ('Pre') sensitivity estimate for each session. Average normalized thresholds (gray markers) reveal enhanced frequency sensitivity during anodal sessions. Error bars indicate standard deviation. **(d)** Group psychometric curves ($n = 15$) from frequency discrimination task (Experiment 4; tDCS over Oz). Conventions as in (a). **(e)** Average frequency sensitivity estimates calculated for individual participants in Experiment 4. Frequency sensitivity did not differ between sham and anodal sessions. Lambda values (inset plot) revealed significant improvement rates that did not differ between sessions. **(f)** Scatter plot shows the relationship between each participant's frequency sensitivity estimates in sham and anodal sessions in Experiment 4. Conventions as in (c). Normalized sigma estimates showed no bias toward better frequency sensitivity with anodal tDCS over Oz compared to sham.

Table 1

Post-stimulation subjective ratings

Expt	Task	tDCS site	Attention			Fatigue			Pain		
			Anodal	Sham	Paired *t*-test	Anodal	Sham	Paired *t*-test	Anodal	Sham	Paired *t*-test
1	Grating orientation	Oz	6.0±0.2	5.6±0.2	*p* = 0.24	3.3±0.4	3.1±0.4	*p* = 0.82	1.8±0.3	1.3±0.2	*p* = 0.09
2		T3	6.4±0.2	5.9±0.3	*p* = 0.11	2.3±0.3	2.1±0.3	*p* = 0.61	1.9±0.2	1.3±0.2	***p* = 0.04**
3	Vibration frequency	Oz	5.8±0.2	5.9±0.2	*p* = 0.33	2.3±0.2	2.4±0.3	*p* = 0.72	1.3±0.3	1.3±0.2	*p* = 0.72
4		T3	5.8±0.2	5.9±0.2	*p* = 0.58	1.7±0.2	2.0±0.3	*p* = 0.48	2.2±0.3	1.7±0.3	*p* = 0.15

Values (mean± SE) indicate participants' responses along a visual analog scale (1–7). A value of 1 indicates poorest attention, minimal fatigue, and minimal pain. A value of 7 indicates maximal attention, maximal fatigue, and maximal pain. *P* values indicate significance of paired t-tests comparing subjective ratings for sham and anodal sessions. Ratings were statistically equivalent between anodal and sham sessions except for pain ratings in experiment 2.